22th_Paper_Nurhasni_Hasan_CP_(2021).pdf

by

Submission date: 04-Apr-2023 03:37PM (UTC+0700)
Submission ID: 2055485803
File name: 22th_Paper_Nurhasni_Hasan_CP_(2021).pdf (4.43M)
Word count: 7788
Character count: 42481

Carbohydrate Polymers 270 (2021) 118387

Contents lists available at ScienceDirect

Carbohydrate Polymers

journal homepage: www.elsevier.com/locate/carbpol

Diethylenetriamine/NONOate-doped alginate hydrogel with sustained nitric oxide release and minimal toxicity to accelerate healing of MRSA-infected wounds

Nurhasni Hasan [a], Juho Lee [a], Dongmin Kwak [a], Hyunwoo Kim [a], Aruzhan Saparbayeva [a], Hye-Jin Ahn [b], In-Soo Yoon [a], Min-Soo Kim [a], Yunjin Jung [a], Jin-Wook Yoo [a,*]

[a] College of Pharmacy, Pusan National University, Busan 46241, South Korea.
[b] School of Mechanical and Aerospace Engineering, Gyeongsang National University, Jinju 52828, South Korea.

ARTICLE INFO

Keywords:
Alginate
Nitric oxide
Hydrogel
Methicillin-resistant *Staphylococcus aureus*
Wound healing

Abstract

This study demonstrates the development of a nitric oxide (NO)-releasing hydrogel wound dressing and its efficacy at accelerating methicillin-resistant *Staphylococcus aureus* (MRSA)-infected wound healing. A DETA/NONOate-doped alginate (Alg-DETA/NO) hydrogel was synthesized using alginate as a hydrogel-forming wound dressing material and diethylenetriamine/diazeniumdiolate (DETA/NONOate) as an NO donor. Alg-DETA/NO exhibited a prolonged NO release profile over a period of 4 days. The rheological properties of Alg-DETA/NO did not differ significantly from those of pure alginate. Importantly, Alg-DETA/NO showed potent antibacterial activity against MRSA, with minimal toxicity to mouse fibroblasts. The application of Alg-DETA/NO to MRSA-infected wounds in a mouse model showed a favorable wound healing with accelerated wound-size reduction and reduced skin bacterial infection. Additionally, histological examination revealed that Alg-DETA/NO reduced inflammation at the wound site and promoted re-epithelialization, angiogenesis, and collagen deposition. Thus, Alg-DETA/NO presented herein could serve as a safe and potent hydrogel dressing for the treatment of MRSA-infected wounds.

1. Introduction

Chronic cutaneous wound infections associated with methicillin-resistant *Staphylococcus aureus* (MRSA) pose a great challenge owing to the difficulties in eradicating MRSA from the wound site. MRSA has developed multiple mechanisms to develop resistance against all conventional antibiotics (Van Bambeke et al., 2008). MRSA can increase the severity of wounds, impair the healing process, and cause high rates of complications such as sepsis and amputation in vascular surgery patients (Albaugh et al., 2013). Therefore, a new generation of antibiotics that do not cause the development of drug resistance while being able to facilitate the healing of MRSA-infected wounds is urgently needed to fight the emergence of MRSA infection.

Nitric oxide (NO), a free radical molecule synthesized from the amino acid L-arginine by three distinct isoforms of NO synthase, has emerged as a new antibacterial agent and a critical small molecule in wound healing (Lee, Kwak, et al., 2020; Nurhasni et al., 2015). NO exhibits broad-spectrum antibacterial effects via multiple biochemical pathways, thereby limiting the resistance-developing ability of bacteria (Privett et al., 2012). These characteristics make NO a suitable candidate for the treatment of MRSA-infected cutaneous wounds. However, the clinical application of NO to wounds is not practical owing to its gaseous nature and very short half-life (2–3 s).

To overcome this limitation, *N*-diazeniumdiolates (NONOates), which are a subset of NO donors characterized by the presence of a diolate group bound to an amine group (nucleophile adduct), have been commonly used as a means for storing and releasing NO to accelerate wound healing in mouse models (Blecher et al., 2012). Among various NONOates, diethylenetriamine (DETA) NONOate is a suitable NO donor due to a very long half-life which can produce continuous and long-lasting NO at the wound site. In addition, its sustained release properties could decrease the frequency of dressing changes, which in turn could accelerate the rate of wound healing and improve patient compliance. Blecher et al. reported that DETA/NONOate accelerated wound healing processes (Blecher et al., 2012). Despite the beneficial properties of DETA/NONOate, however, a harmful nitrosamine

* Corresponding author at: College of Pharmacy, Pusan National University, Busan 609-735, South Korea.
E-mail address: jinwook@pusan.ac.kr (J.-W. Yoo).

https://doi.org/10.1016/j.carbpol.2021.118387
Received 28 April 2021; Received in revised form 12 June 2021; Accepted 27 June 2021
Available online 1 July 2021

byproduct (i.e., DETA) which is produced by the NO released from DETA/NONOate is a main hindrance to clinical applications. DETA is a corrosive chemical that can severely irritate and burn the skin (Hudson, 2020; Kröncke & Suschek, 2008). Thus, a novel strategy that can mitigate DETA/NONOate toxicity without negatively affecting the sustained NO release is needed for safe and effective use of DETA/NONOate in the treatment of cutaneous wounds.

Alginate is a water-soluble anionic biocompatible polysaccharide, comprising 1,4-linked-α-L-guluronic acid and β-D-mannuronic acid residues that can be conveniently modified at the hydroxyl and carboxylic acid functional groups (Cao et al., 2020; Oshi et al., 2018). Alginate has been widely used as a major component of various wound dressings because it forms a hydrogel with a high-water absorption capacity and hemostatic properties and disintegrates into biodegradable monosaccharide residues upon coming in contact with wound fluids without enzyme addition (Blaine, 1947; Shrestha et al., 2020). Interestingly, it has been found that alginate–drug conjugates can mitigate drug toxicity. Tian, Chen, Gu, et al., 2016 and Tian, Chen, Li, et al., 2016. showed that deferoxamine toxicity was reduced in alginate–deferoxamine conjugates whose increased molecular size prevented their diffusion into the cell (Tian, Chen, Gu, et al., 2016; Tian, Chen, Li, et al., 2016). Furthermore, it has been found that NO release can be prolonged by the conjugation of NONOates and macromolecules owing to slow degradation of the macromolecules (Miller & Megson, 2007). Based on these findings, we hypothesized that conjugation of alginate to DETA/NONOate would minimize the potential DETA toxicity by preventing its direct exposure of the skin while maintaining hydrogel-forming and sustained NO release properties.

Herein, we report the development of a DETA/NONOate-doped alginate (Alg-DETA/NO) hydrogel for the treatment of MRSA-infected cutaneous wounds. After confirming its successful synthesis, Alg-DETA/NO was tested for in vitro NO release, rheological properties, in vitro cytotoxicity, and in vitro and in vivo efficacy against MRSA. Additionally, the in vivo wound-healing activity was evaluated in MRSA-infected wounds. We also evaluated the mechanisms through which Alg-DETA/NO accelerates MRSA-infected wound healing by assessing myeloperoxidase (MPO) activity and performing histopathological analysis (hematoxylin and eosin [H&E], Masson's trichrome [MT], and Gram staining and CD31 immunostaining).

2. Materials and methods

The methods of characterization of Alg-DETA/NO, in vitro NO release study, fluid uptake study, rheological properties, in vitro antibacterial activity and cytotoxicity, histology and immunohistochemistry, collagen assay, determination of wound bacterial burden, MPO assay, and statistical analyses are provided in the Supplementary Information.

2.1. Materials

Alginic acid sodium salt from brown algae (Mw range of 100,000–120,000, with a mannuronate/guluronate ratio of 1.56), DETA, 1-ethyl-3-(3-dimethylaminopropyl)carbodiimide hydrochloride (EDC), N-hydroxysuccinimide (NHS) sodium methoxide ($NaOCH_3$), the tetrazolium dye 3-(4,5-dimethylthiazol-2-yl)-2,5 diphenyltetrazolium bromide (MTT), Mayer's hematoxylin, eosin-Y disodium salt, hexadecyltrimethylammonium bromide (HTAB), 2,2,2-tribromoethanol, tert-amyl alcohol (2-methyl-2-butanol), the Griess assay reagent, o-dianisidine dihydrochloride, and dimethylsulfoxide were purchased from Sigma-Aldrich (St. Louis, MO, USA). The NO and nitrogen (N_2) gasses were obtained from HANA Gas (Gimhae, South Korea). Bacto™ tryptic soy broth medium was purchased from BD Biosciences (Sparks, MD, USA). MT stain, anti-CD31 antibody, and goat anti-rabbit IgG H&L (HRP) were purchased from Abcam (Cambridge, MA, USA). The soluble collagen assay kit was purchased from Cell Biolabs, Inc. (San Diego, CA, USA). Roswell Park Memorial Institute (RPMI) 1640 medium, trypsin, fetal bovine serum, and penicillin-streptomycin were procured from HyClone, Thermo Fisher Scientific Inc. (Waltham, MA, USA). Phosphate-buffered saline (PBS; 20×) was purchased from Biosesang (Seoul, South Korea). All other reagents and solvents were of analytical grade.

2.2. Synthesis of Alg-DETA/NO

DETA was covalently attached to alginate before Alg-DETA/NO synthesis, according to a previously reported method, with slight modifications (Ahonen et al., 2018; Cao et al., 2019) (Fig. 1). Alginate (1 g) and EDC (final concentration of 50 mM) were dissolved in 100 mL of demineralized water, and the reaction was allowed to proceed for 1 h. DETA was added dropwise to the alginate mixture (polymer:DETA, weight ratio of 2:1) and the pH was adjusted to 4.0 with 1 M HCl. The reaction mixture was incubated under constant stirring at 25 °C overnight. On the next day, the amine-modified alginate was precipitated with anhydrous ethanol, and after filtration, the precipitate was washed twice with anhydrous ethanol, followed by overnight vacuum drying to obtain a white Alg-DETA solid.

To synthesize Alg-DETA/NO, a solution of functionalized alginate (1.5 g of Alg-DETA) in dry methanol (10 mL) and 50 mM NaOH (80 mL) was prepared; then, $NaOCH_3$ (1 mol equiv. with respect to the total amine sites) in dry methanol (10 mL) was added to the Alg-DETA solution, and the mixture was placed in a Parr high-pressure reactor. The high-pressure reactor was flushed three times with 20 psi $Ar_{(g)}$ for 15 min to remove oxygen and subsequently charged with $NO_{(g)}$ at 80 psi at 25 °C for 3 days. Then, NO was vented, and the reactor was flushed with 20 psi $Ar_{(g)}$ for 15 min to remove unreacted NO. The final product was precipitated with cold anhydrous ethanol, filtered, and vacuum-dried overnight to obtain a light-yellow solid. The product was stored at −20 °C for up to 6 months before use.

2.3. In vivo wound healing activity

Male ICR mice (7–8 weeks old, Samtako Bio Korea, Osan, South Korea) were used in this study. All animal experiments were performed in accordance with the regulations of Korean Legislation on animal studies and were approved by the Ethical Scientific Committee of Pusan National University. Before the introduction of wounds on the dorsal area, mice were anesthetized via intraperitoneal injection of 2% solution of tribromoethanol (15 μL per gram of body weight). The dorsal hair was shaved using an electric razor, and the back skin was excised using an 8-mm biopsy punch to create full-thickness wounds. Thereafter, the wounds were inoculated with a bacterial suspension (60 μL) containing 1×10^7 CFU/mL of MRSA (USA300) FPR3757 (GenBank accession no. NC_007793) to induce infection. Alg, Alg-DETA, and Alg-DETA/NO (10 mg) were topically applied from day 2 post-injury, when signs of infection were obvious. Each wound was covered with sterile gauze. Untreated mice were used as a control. Photographs of the wounds were taken to observe the gross visual wound healing based on the wound area not covered by migrating epithelial cells. ImageJ (National Institutes of Health, Bethesda, MD, USA) was used to determine the reduction in the wound size, which was calculated as follows:

$$\text{Wound size reduction } (\%) = \frac{Wt}{Wo} \times 100$$

where W_0 is the initial wound area at time 0 and W_t is the wound area at time t.

3. Results and discussion

3.1. Synthesis of Alg-DETA/NO and quantification of the NO content

Alginate–DETA conjugation was completed before the synthesis of

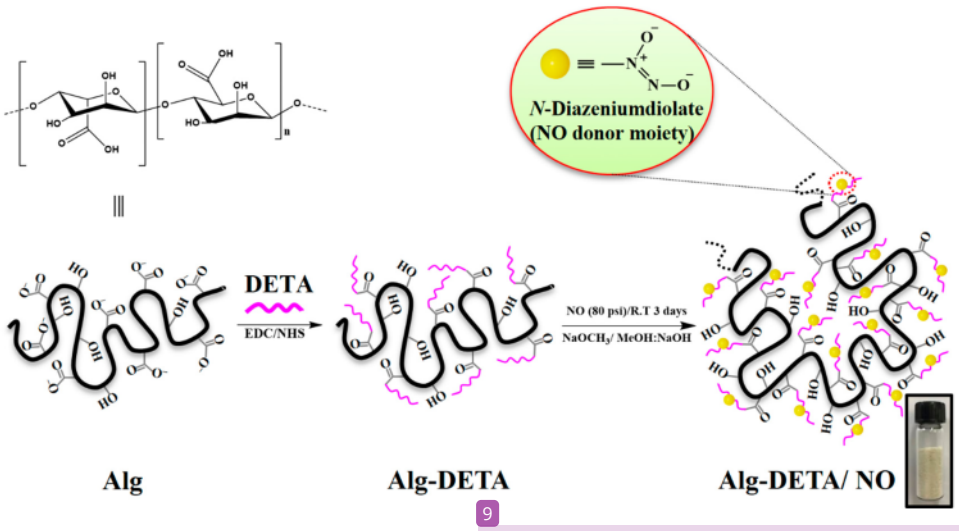

Fig. 1. Synthesis of Alg-DETA/NO. Alg, alginate; DETA, diethylenetriamine; EDC, 1-ethyl-3-(3-dimethylaminopropyl) carbodiimide hydrochloride; NHS, N-hydroxysuccinimide; NO, nitric oxide; R.T, room temperature; $NaOCH_3$, sodium methoxide.

Alg-DETA/NO (Fig. 1). The carboxylic groups of the alginate and the amine groups of DETA were covalently linked by carbodiimide coupling. The amide bond formed between the alginate polymer and DETA provides many secondary amine sites. The secondary amine group of Alg-DETA then reacts with $NO_{(g)}$ under high pressure (80 psi) to create a relatively stable NONOate (NO donor) structure with alginate polymer as the backbone.

The ultraviolet-visible (UV–Vis) spectra were measured under various conditions to characterize Alg-DETA/NO as an NO donor. The presence of the NONOate group was confirmed by the characteristic absorption peak at 260 nm (Fig. 2A, red line), while Alg-DETA did not show a peak at 260 nm (Fig. 2A, black line). The absorption of Alg-DETA/NO measured at 260 nm decreased in a concentration-dependent manner, further confirming the presence of the NONOate (Fig. 2B). Infrared measurements also confirmed the presence of the NONOate functional group in the Alg-DETA/NO polymer (Fig. S1). The Alg-DETA/NO spectrum exhibited a characteristic NONOate peak at 1238 cm^{-1}, which was absent in the Alg, DETA, and Alg-DETA spectra (Wan et al., 2008). In addition, the characteristic functional groups of Alg, DETA, and Alg-DETA are still detected in the infrared spectra. The typical infrared spectrum of alginate has the following absorption bands: a broad band at 3397 cm^{-1} (O—H stretching); medium bands at 2923 and 2853 cm^{-1} (C—H stretching); strong bands at 1601 and 1460 cm^{-1} (C═O stretching); a medium band at 1089 cm^{-1} (alkoxy C—O stretching); and a medium band at 1302 cm^{-1} (aromatic ester C—O stretching). In the DETA absorption spectrum, the medium band at 3354 cm^{-1} is assigned to the stretching vibration of the N—H bond. The primary amine C—N stretching was visible at 1062 cm^{-1}, and the strong band at 1127 cm^{-1} was attributed to the stretching of the secondary amine group C_2—N. The medium bands at 2926 and 2854 cm^{-1} were assigned to the stretching vibration of C—H bonds. The 1354 cm^{-1} band represented the bending of C—H_2 bonds. The infrared spectrum of Alg-DETA showed characteristic absorption bands of both alginate and DETA. A typical infrared spectrum of Alg-DETA has the following absorption bands: a broad band at 3335 cm^{-1} (N—H stretching, O—H stretching); medium bands at 2923 and 2853 cm^{-1} (C—H stretching); strong bands at 1579 and 1460 cm^{-1} (C═O stretching); a strong band at 1376 cm^{-1} (C—H bending); a medium band at 1070 cm^{-1} (C—N stretching); and a medium band at 1250 cm^{-1} (aromatic ester C—O stretching). Although the N—H stretching vibration at 3335 cm^{-1} in DETA was overlapped by the broad O—H stretching band of the hydroxyl groups in Alg, strong bands of the C—H stretching were observed in the Alg–DETA conjugate at 2923 and 2853 cm^{-1}. Thus, these results confirmed the successful conjugation of alginate and DETA (*Infrared Spectroscopy Absorption Table*, 2020).

The conjugation between Alg-DETA and NO was verified using proton nuclear magnetic resonance (^{1}H NMR; Fig. S2). The ^{1}H NMR details of Alg-DETA are as follows: (D2O, 500 MHz, δ) 2.43–3.47 [OCNHC*H*$_2$CH$_2$, OCNHCH$_2$C*H*$_2$, NHC*H*$_2$NH$_2$, NHCH$_2$C*H*$_2$NH$_2$], 3.65–4.19 [C2, C3: OCHCH(*OH*)C*H*(OH), OCHC*H*(*OH*)CH(OH)], 4.47 [C4: OC*H*CH(*OH*)CH(OH)], 4.63–4.71 [C5: OHCOC*H*], 4.87 [C1: OC*H*(CHOH)O] (Beauchamp, 2010). The proton signals of the methylene groups near the secondary amine sites of Alg-DETA at 2.8 ppm were shifted to 2.73 ppm in Alg-DETA/NO as a result of the electron-withdrawing effect of the NONOate group.

The Griess assay was performed to measure the amount of NO in the polymer. Auto-oxidation of NO released from Alg-DETA/NO (NO^{2-}) can result in the production of an azo dye in the presence of Griess reagent; the dye shows a characteristic peak in the UV–Vis spectrum at 540 nm. Alg-DETA/NO exhibited a peak at 540 nm upon reacting with the Griess reagent (Fig. 2A, green line). The Griess assay (Vis spectrum), as well as the aforementioned results (UV, FTIR, and NMR spectra), all confirmed the formation of the NONOate group. Before NO measurement using the Griess assay, Alg-DETA/NO was incubated with citrate buffer (pH 4.0) to accelerate the complete release of NO, which was confirmed by the absence of a peak corresponding to NO in the UV–Vis spectrum at 260 nm. The amount of NO in Alg-DETA/NO was 0.23 μmol/mg polymer (Table 1).

3.2. Study of in vitro NO release

The NO release profile of Alg-DETA/NO in PBS (pH 7.4, 37 °C was measured using a chemiluminescence NO analyzer. A real-time NO release profile for the first 10 h is shown in Fig. 2C, and a plot of the percentage and amount of NO released over time is shown in Fig. 2D. The real-time NO-release graph shows that the maximum flux of NO was 27 ppb/mg Alg-DETA/NO. Alg-DETA/NO displayed a prolonged release of NO over a period of 4 days (Fig. 2D), with a half-life ($t_{1/2}$) of ~13 h at pH 7.4, 37 °C (Table 1). Interestingly, our novel synthesized NONOates showed a remarkably longer half-life than those of other NO donors in the same class, such as 1-[2-(carboxylate)pyrrolidine-1-yl] NONOate (PROLI/NO, $t_{1/2} \approx 2$ s), methylamine hexamethylene methylamine

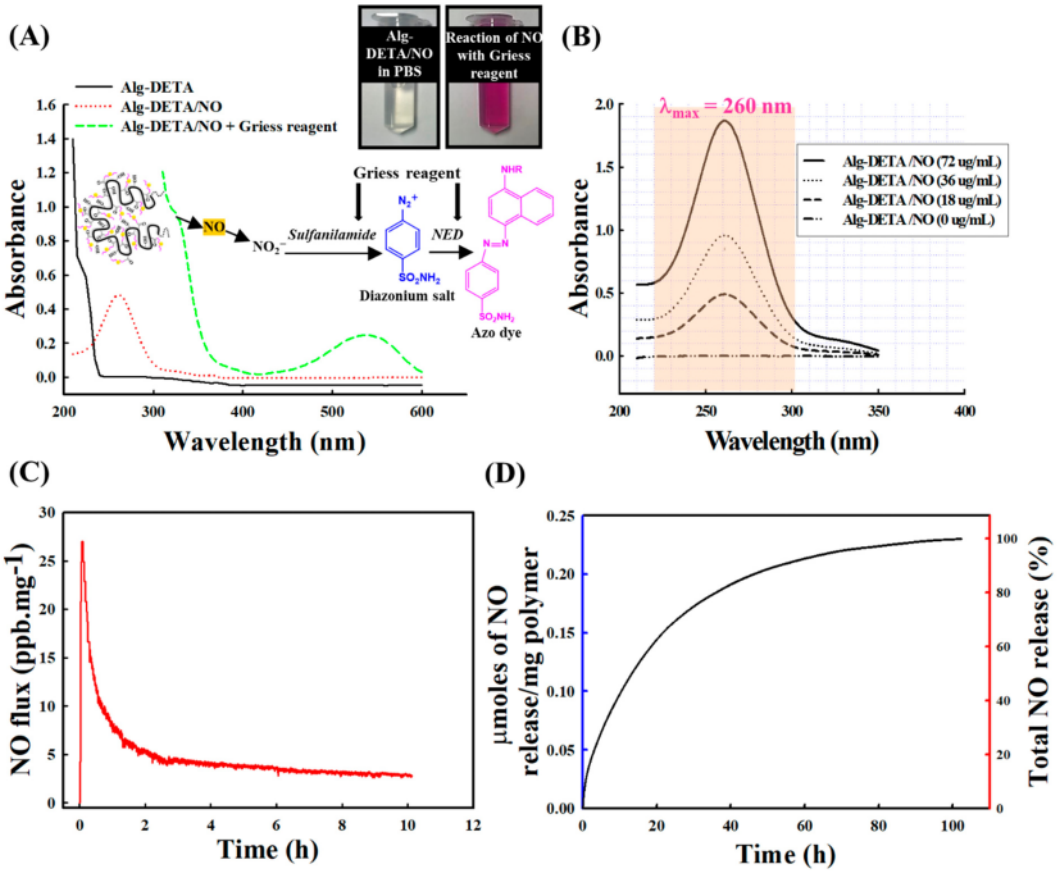

Fig. 2. Characterization of Alg-DETA/NO. (A) UV–Vis absorption spectra of Alg-DETA/NO (red dotted line), Alg-DETA/NO with the Griess reagent (green dashed line), and Alg-DETA (black line). (B) UV–Vis spectra of Alg-DETA/NO at different concentrations. (C) Real-time NO release in the first 10 h. (D) Percentage of the total NO released and the amount of NO released over time in PBS (pH 7.4, 37 °C) measured using a Sievers 280i chemiluminescence NO analyzer. Alg, alginate; DETA, diethylentriamine; NO, nitric oxide.

Table 1
NO-release properties of Alg-DETA/NO in PBS (pH 7.4, 37 °C).

NO donor	t[NO][a] (μmol/mg)	$[NO]_{max}$[b] (ppb/mg)	$t_{1/2}$[c] (h)	t_d[d] (h)
Alg-DETA/NO	0.23 ± 0.006	27.02 ± 3.107	13.35 ± 0.066	102.40 ± 0.003

Values are expressed as the mean ± standard deviation of three independent measurements.
[a] Total NO released.
[b] Maximum flux of NO release.
[c] NO-release half-life.
[d] Duration of NO release.

NONOate (MAHMA/NO, $t_{1/2}$ ≈ 1 min), diethylamine NONOate (DEA/NO, $t_{1/2}$ ≈ 2 min), propylamine propylamine NONOate (PAPA/NO, $t_{1/2}$ ≈ 15 min), spermine NONOate (SPER/NO, $t_{1/2}$ ≈ 6 min), and dipropylentriamine NONOate (DPTA/NO, $t_{1/2}$ ≈ 3 h) (Keefer, 2005). The presence of the alginate backbone in our synthesized NONOate could have contributed to its longer half-life. The chemical modification at the hydroxyl and carboxylic acid functional groups of alginate may alter the solubility and degradation rate of the final product (Bernkop-Schnürch et al., 2001). However, Alg-DETA/NO exhibited a relatively stable NO release without an initial burst (Fig. 2D). It released ~68% of NO in the first 24 h and 88% over 48 h, followed by a gradual sustained release over 4 days. This profile can reduce the frequency of Alg-DETA/NO application to the wound (e.g., every 2 days) while maintaining the appropriate dose of NO. Frequency dressing changes are associated with an increased incidence of wound sepsis and delayed wound healing (Wynne et al., 2004). Therefore, our synthesized Alg-DETA/NO polymer, which releases NO in a sustained manner, can overcome these potential problems.

3.3. Fluid uptake and rheological properties

The Alg-DETA/NO dressing forms a hydrogel upon contact with a wound exudate. Therefore, the fluid uptake ability was investigated to measure the maximum swollen condition. The swelling of the Alg-DETA/NO powder by absorption of the simulated wound fluid (SWF) further facilitated drug release. Alg-DETA/NO rapidly absorbed SWF, up to approximately 1000% and 2183% of its own mass in SWF within 1.5 and 4.5 h, respectively (Fig. 3A). After the initial rapid absorption of SWF, the fluid uptake by Alg-DETA/NO slowed down, reaching approximately 2200% at 5.5 h with no significant fluid absorption observed afterward. The fluid uptake profiles of Alg, Alg-DETA, and Alg + DETA/NO (physical mixture 1:1) showed no significant differences from that observed in Alg-DETA/NO. The hydrogen bonds formed between alginate and water molecules enabled the SWF to be trapped in

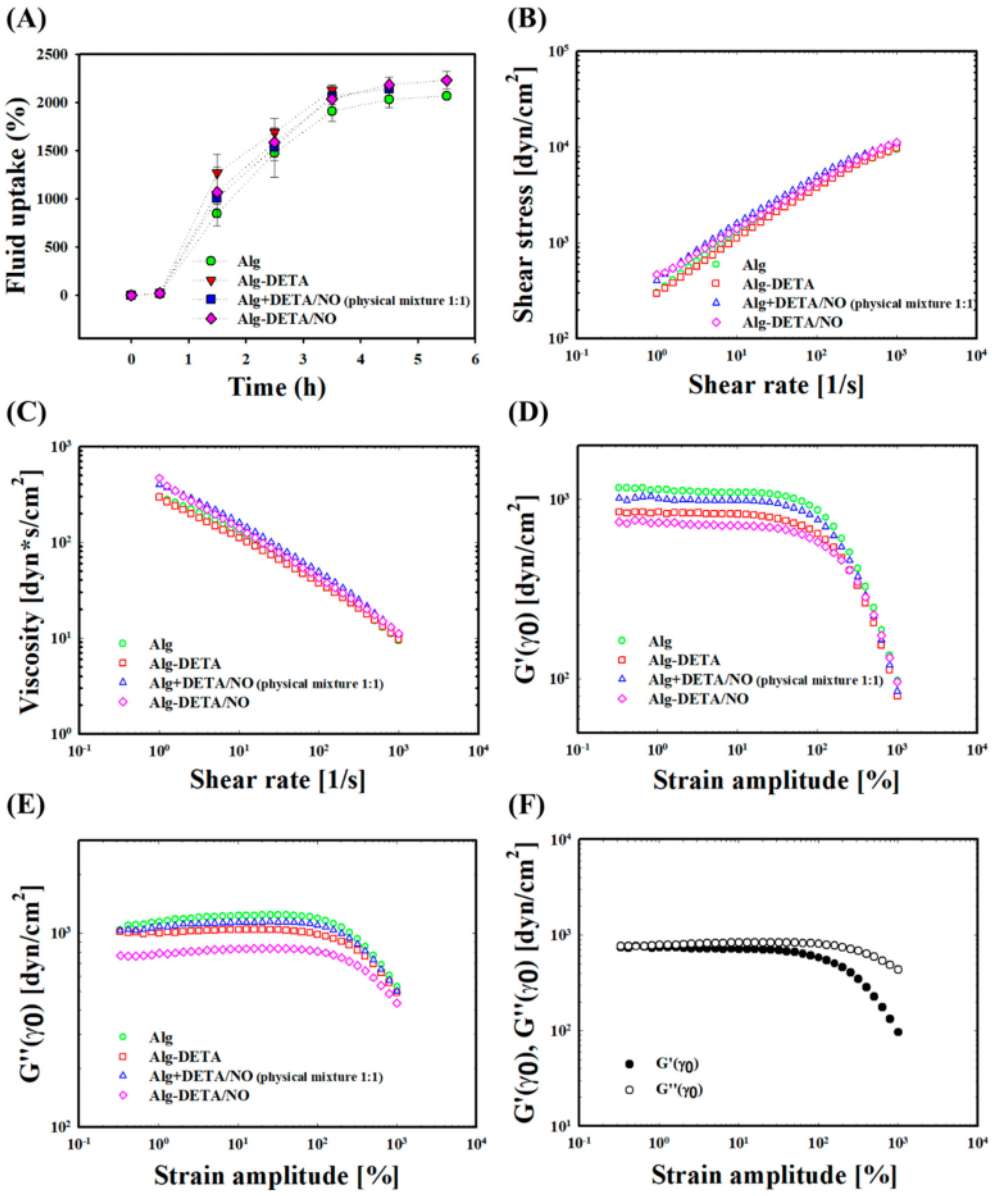

Fig. 3. Fluid uptake and rheological properties of test samples. (A) Simulated wound fluid uptake profiles of Alg, Alg-DETA, Alg + DETA/NO (physical mixture 1:1), and Alg-DETA/NO presented as a percentage of the weight gained via fluid uptake relative to the initial weight of the polymers. (B) Shear stress of the samples following SWF absorption at the maximum swollen condition per weight as a function of the shear rate. (C) Viscosity vs. shear rate. (D) Storage modulus (G') and and (E) loss modulus (G'') of each maximum swollen condition as a function of the strain amplitude. (F) G' and G'' of Alg-DETA/NO swollen by 2200% as a function of the strain amplitude. Alg, alginate; DETA, diethylentriamine; NO, nitric oxide.

the intermolecular space of the hydrogel structure. After the intermolecular space is filled with SWF, no more fluid can be absorbed, thus reaching the maximum swollen condition (Lee, Hlaing, et al., 2019; W. Y. Lee, Asadujjaman, & Jee, 2019).

The rheological profiles of the test samples are shown in Fig. 3B–F. All samples presented shear thinning with a pseudoplastic flow behavior (Fig. 3B). At a low shear rate, the alginate-based hard inner gel structure showed a high shear viscosity as it resisted flow; however, when the shear rate increased, the internal structure collapsed, resulting in a rapid decrease in the resistance and, accordingly, a decrease in the shear viscosity (Fig. 3C). When applied, pseudoplastic materials have a relatively low viscosity, suggesting that they can spread out relatively smoothly. Thus, Alg-DETA/NO could maintain a gel-like structure and resist small shear stresses, such as the gravitational force or brushing against a secondary dressing. These characteristics are desirable as wound dressings should be able to maintain enough viscosity at the wound site to avoid excessive flow (Matthews et al., 2006). Fig. 3D–F shows the storage modulus (G') and loss modulus (G'') graphs as a function of the strain amplitude at the maximum swollen condition of each alginate-based sample at a fixed angular frequency (ω) of 10 rad/s.

All four samples showed relatively small strain amplitudes and exhibited a slightly dominant (liquid-like) G''; however, when the strain amplitude exceeded 10 to 30% because of the structure destruction, both G' and G'' showed a decreasing shear-thinning behavior. At this point, owing to the destruction of the internal network of the material, the storage elastic modulus, which is a measure of the solid property of the material, rapidly decreased. The more the structure of the material is destroyed, the more the material tends to exhibit a superior liquid behavior. Thus, the Alg-DETA/NO hydrogel could easily flow and be removed from the wound site. Notably, the rheological properties of the Alg-DETA/NO conjugate did not differ significantly from those of pure alginate.

3.4. In vitro anti-MRSA activity

Antibacterial agents with high bactericidal activity are needed to overcome the emergence of bacterial resistance (Stratton, 2003). The antibacterial activity of Alg-DETA/NO against MRSA was evaluated by counting the number of colony-forming units (CFU) of MRSA and assessing the ability of Alg-DETA/NO to exhibit >6-log killing (i.e., a 99.9999% reduction) of MRSA. In vitro antibacterial activities of Alg-DETA/NO at different concentrations (5, 10, 20, and 40 mg/mL) and incubation times (24 and 36 h) are shown in Fig. 4. Alg-DETA/NO killed MRSA in a concentration- and time-dependent manner. After 24 h of incubation, approximately 3-log killing (99.9% reduction) and ~4-log killing (99.99% reduction) of MRSA were observed at Alg-DETA/NO concentration of 20 and 40 mg/mL, respectively, whereas at concentrations of 5 and 10 mg/mL, Alg-DETA/NO reduced the number of viable bacterial cells by ~90% and 99%, respectively. Furthermore, as the incubation time was extended to 36 h, the antibacterial effect of Alg-DETA/NO increased at all concentrations. A 99% reduction in the number of viable bacterial cells (2-log killing) was observed at a concentration of 5 mg/mL Alg-DETA/NO, whereas at concentrations of 10, 20, and 40 mg/mL, Alg-DETA/NO reduced the number of viable bacterial cells by 99.9% (3-log killing), 99.999% (5-log killing), and 99.9999% (>6-log killing), respectively. By contrast, alginate and Alg-DETA did not show antibacterial activities even at high concentrations (up to 40 mg/mL). Thus, the NO released from Alg-DETA/NO was the key factor in killing MRSA. Reactive N_2 species derived from NO and superoxide ($O_2^{\bullet-}$) have been reported to kill MRSA via several proposed mechanisms, such as cell wall damage and lysis and the modification of DNA, proteins, and lipids, or indirectly via modification of the immune response or other host cell functions (Fang, 1997; Hlaing et al., 2018). In vitro release experiments revealed that 68% of NO was released in the first 24 h, indicating the potent bactericidal effect of Alg-DETA/NO. With a remarkable 4-log killing of resistant bacteria using less NO, our system presents a promising approach to eradicating MRSA infection from the wound area, leading to the acceleration of the healing process.

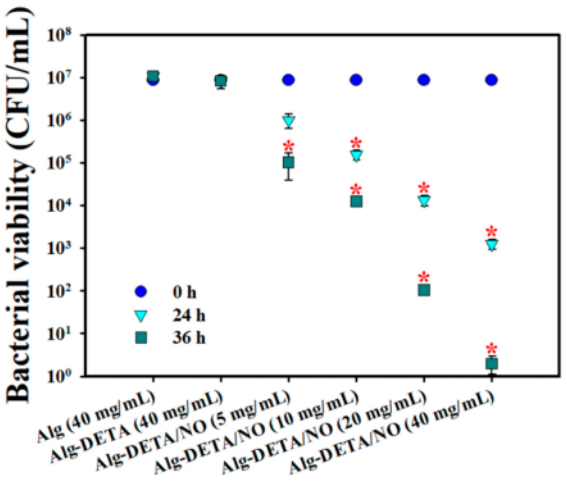

Fig. 4. Antibacterial activities of Alg, Alg-DETA, and Alg-DETA/NO against MRSA. Data are the mean ± standard deviation ($n = 3$). *$P < 0.05$, compared with the Alg (40 mg/mL) group. Alg, alginate; DETA, diethylenetriamine; NO, nitric oxide; MRSA, methicillin-resistant *Staphylococcus aureus*; CFU, colony-forming units.

3.5. In vitro study of Alg-DETA/NO cytotoxicity toward mouse fibroblasts

The viability levels of L929 mouse fibroblasts after exposure to various concentrations of test samples are shown in Fig. 5. Alginate and Alg-DETA/NO elicited no significant cytotoxicity (>80% cell viability) at concentrations of 1.25 to 40 mg/mL, whereas Alg-DETA showed similar results only at a concentration of 2.5 mg/mL. Alg-DETA exhibited a weak cytotoxicity (>60% cell viability) toward L929 mouse fibroblasts at concentrations of 5 to 40 mg/mL. In contrast to alginate and Alg-DETA/NO, DETA, DETA/NO, and Alg + DETA/NO (physical mixture 1:1) showed significant toxicities (cell viabilities <60%) toward L929 mouse fibroblasts, regardless of the polymer concentration. Thus, conjugation of alginate to alkyl amines and a subsequent attachment of NO to the secondary amine indirectly influenced the cytotoxicity of the polymers. In general, Alg-DETA/NO was less toxic than the control. Tian, Chen, Li, et al. (2016) reported that the conjugation of alginate to the amine-based toxic agent (deferoxamine) reduced the cytotoxicity of the drug because the increased molecular size could prevent the diffusion of the conjugate into cells (Tian, Chen, Li, et al., 2016). Moreover, NO itself has been reported to increase fibroblast proliferation (Gansauge et al., 1997).

Compared with that of commercially available topical antiseptics and other NO-releasing systems, the in vitro toxicity of Alg-DETA/NO toward L929 mammalian fibroblasts was very low. Povidone-iodine and chlorhexidine, two well-known topical antiseptics, significantly reduced the viability of human fibroblasts, to less than 10% (Balin & Pratt, 2002; Pyo et al., 1995; Sun et al., 2012). Despite their extremely high in vitro cytotoxicity, povidone-iodine and chlorhexidine are commonly used in clinical settings because they can effectively reduce infection and promote wound healing (White et al., 2006). Thus, the negligible toxicity of Alg-DETA/NO toward L929 mammalian fibroblasts supports its potential use for the treatment of bacteria-infected wounds, showing that our NO-releasing alginate is suitable for topical application as a wound-healing agent for the treatment of MRSA-infected wounds.

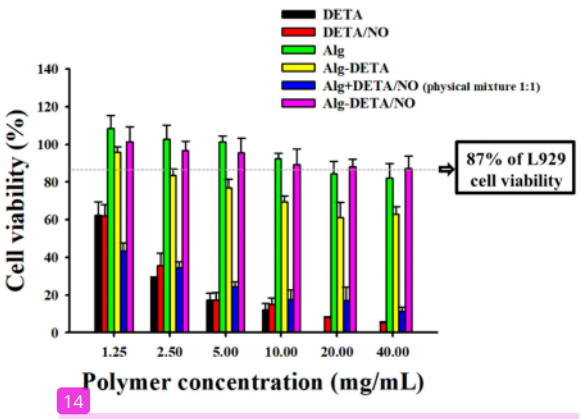

Fig. 5. Viability of L929 mouse fibroblasts after 24-h exposure to different concentrations of test samples ($n = 8$). Alg, alginate; DETA, diethylenetriamine; NO, nitric oxide.

3.6. Wound-healing activity of Alg-DETA/NO in a mouse model of MRSA-infected wounds

The wound-healing activity of Alg-DETA/NO was evaluated in a mouse model of MRSA-infected wounds (Fig. 6). As the skin on the back of a mouse is loose and elastic, it can reduce the tension around wounds, which can in turn accelerate the wound contraction. To reduce the impact of this limitation, Tegaderm™ was used to fix the skin and prevent skin contraction (Bae et al., 2012). Subsequently, wounds were treated with Alg-DETA/NO once every 2 days based on its in vitro NO release profile, and an in vivo wound healing assay was performed to investigate whether Alg-DETA/NO can accelerate the repair of MRSA-infected wounds by eradicating skin infection and promoting wound healing. Measurement of the percentage of the wound area revealed that the Alg-DETA/NO-treated group showed greater eradication of skin infection and higher wound-healing activity than the untreated and Alg- and Alg-DETA-treated groups. After day 6 post-injury, the Alg-DETA/NO-treated group showed progressive reduction in skin infection and enhanced wound healing. By contrast, the untreated and Alg- and Alg-DETA-treated groups showed neither reduction in wound bacterial burden nor wound healing (Fig. 6A). These findings confirmed that uncontrolled bacterial colonization on the surface of the wound and in the adjacent tissue might affect or delay the healing process from inflammation to the remodeling phase. Accordingly, after reduction in the bacterial burden, the rate of healing significantly increased, with a reduction in the wound size from 30 to 96% ($P < 0.05$) between days 6 and 12 post-injury (Fig. 6B). Importantly, treatment with Alg-DETA/NO resulted in nearly complete wound closure (96% wound size reduction; $P < 0.05$) and clear epithelialization without any scab on day 12 post-injury (Fig. 6A), confirming the role of NO in the wound healing process. NO is well studied as a potent mediator of angiogenesis, cell proliferation, wound contraction, and collagen formation (Choi et al., 2020; Lee, Hlaing, et al., 2020). Overall, the bactericidal effect and wound-healing activity of NO facilitate the treatment of MRSA-infected wounds.

3.7. Immunohistochemical and histological examination of MRSA-infected wounds

Immunohistochemical and histological examination provided insights into the molecular mechanisms of Alg-DETA/NO-mediated healing of MRSA-infected wounds in the mouse model. The formation of blood vessels was examined using immunohistochemical staining for CD31, while the skin layer morphology and collagen deposition were evaluated using H&E and MT staining, respectively. CD31 is a well-defined marker for blood vessel formation which is highly expressed on the surface of endothelial cells (Kim et al., 2009; Schlüter et al., 2018). CD31 immunostaining and H&E staining of wounded skin tissues were performed on days 6 and 12 post-injury, whereas MT staining was performed on day 12 post-injury. Alg-DETA/NO increased angiogenesis by inducing the formation of new blood vessels on day 6 post-injury and the maturation of blood vessels on day 12 post-injury (Fig. 7A, CD31 staining). By contrast, the untreated and Alg- and Alg-DETA-treated

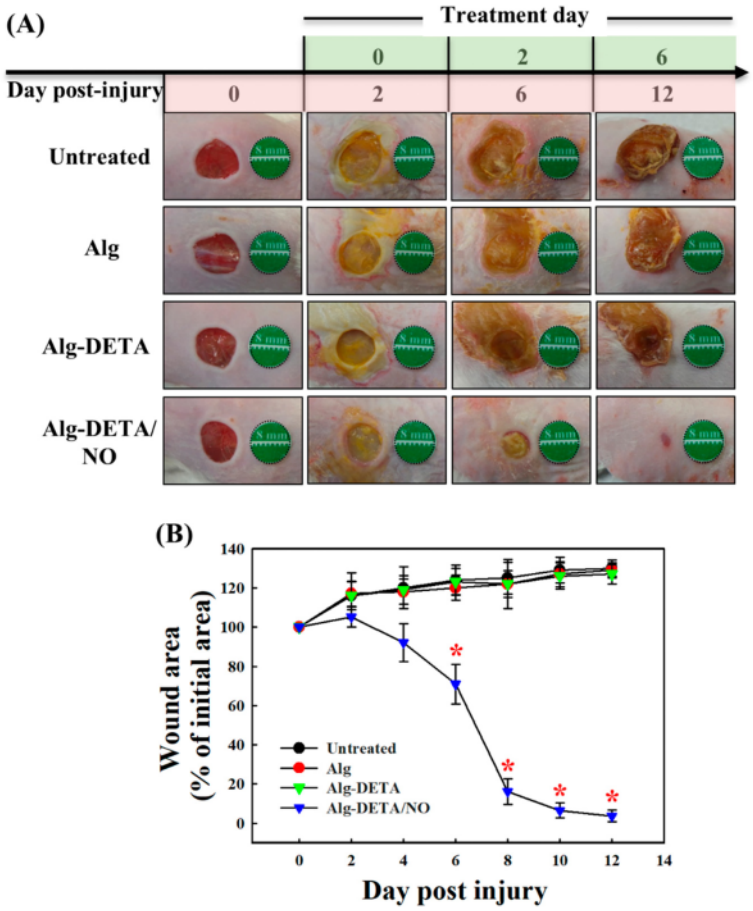

Fig. 6. Effect of test samples on the healing of methicillin-resistant *Staphylococcus aureus* (MRSA)-infected wounds in ICR mice. (A) Representative photographs of the healing of MRSA-infected wounds treated with or without Alg-DETA/NO (5 mg). (B) Percentage of the area reduction of mouse skin lesions relative to the initial 8-mm wound. Data are the mean ± standard deviation ($n = 10$); *$P < 0.05$, compared with the untreated group. Alg, alginate; DETA, diethylenetriamine; NO, nitric oxide.

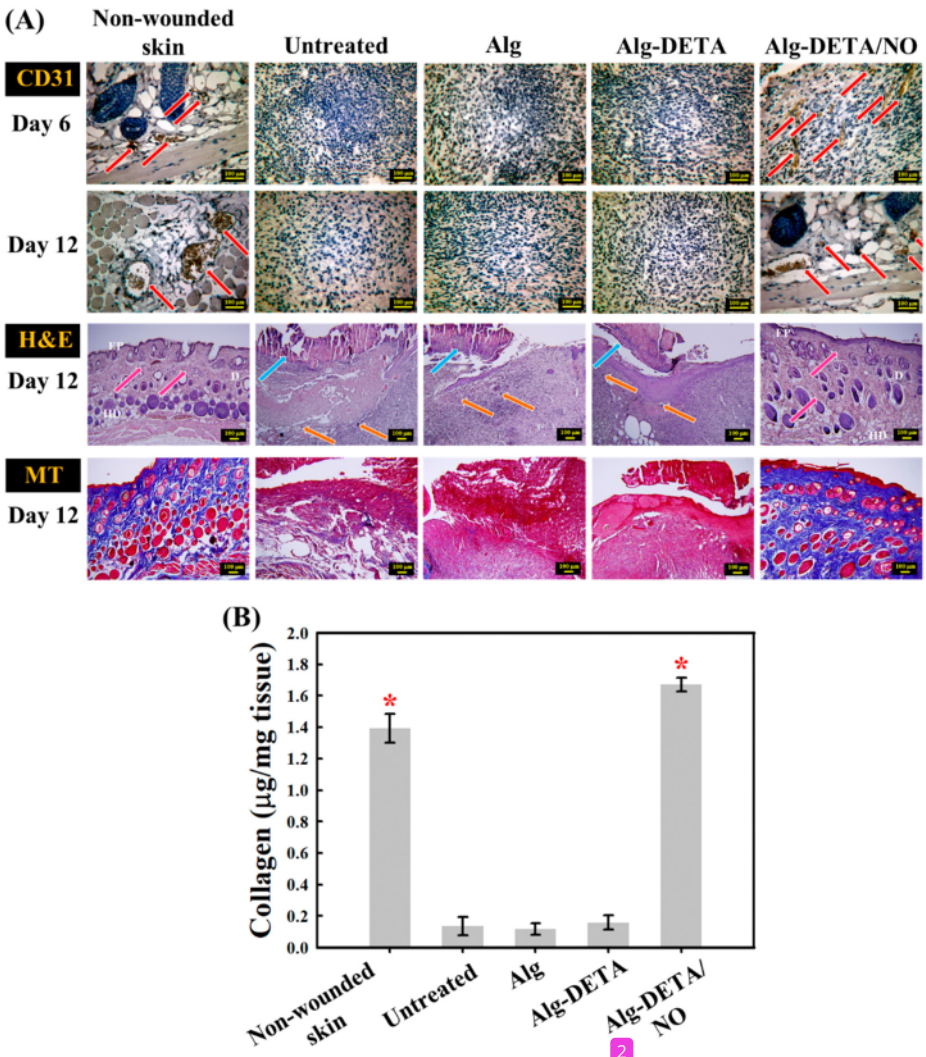

Fig. 7. (A) Immunohistochemical staining for CD31 and histological (H&E and MT staining) analysis of Methicillin-resistant *Staphylococcus aureus*-infected wounds in ICR mice. Scale bar = 100 μm; Ep, epidermal; D, dermal junction; HD, hypodermis; H&E, hematoxylin and eosin; MT, Masson's trichrome. Red arrows indicate blood vessels; blue arrows indicate early epithelialization, pink arrows indicate fibroblasts, and orange arrows indicate mononuclear inflammatory cells. The blue color in the MT-stained tissue indicates collagen, arranged parallel to the skin surface. (B) Collagen amount in wound tissues on day 12 post-injury. Data are the mean ± standard deviation ($n = 3$). *$P < 0.05$, compared with the untreated group. Alg, alginate; DETA, diethylenetriamine; NO, nitric oxide.

groups did not show any signs of angiogenesis. Fig. S3 and Fig. 7A (H&E staining) show the healing progress of the skin. On day 6 post-injury, all samples showed the formation of granulation tissues. However, the Alg-DETA/NO-treated samples showed reduced levels of granulation tissue with a thin immature epithelium. These samples also showed the formation of new blood vessels. By day 12 post-injury, the wound tissues from the Alg-DETA/NO-treated group showed a markedly increased number of fibroblast-like cells and a decreased number of mononuclear inflammatory cells; moreover, the healed skin structure was very similar to that of the healthy non-wounded skin. Meanwhile, the untreated and Alg- and Alg-DETA-treated groups showed open wounds and early epithelialization, ulceration, and the abundance of mononuclear inflammatory cells with deep inflammatory infiltration through the dermal layer. MT staining showed significantly higher collagen deposition in the Alg-DETA/NO-treated group than in the other groups (Fig. 7A). These results were consistent with those of collagen measurements shown in Fig. 7B; the collagen amount in the Alg-DETA/NO-treated group was significantly higher ($P < 0.05$) than those in the untreated and Alg-, and Alg-DETA-treated groups. The effect of NO on collagen formation may primarily be due to the inhibition of collagen degradation by MRSA in the infected tissue or to the increase in collagen synthesis, rather than to de novo transcription of the pertinent collagen genes (Hasan et al., 2019; Martinez et al., 2009). Thus, Alg-DETA/NO accelerated wound healing via different mechanisms that targeted different phases of wound healing.

3.8. Anti-inflammatory and anti-MRSA activities of Alg-DETA/NO in vivo

Bacterial colonization in a wound interrupts the healing process. Thus, removal of the infectious agent from the wound bed is necessary to prevent severe local and systemic infection, thereby improving the

wound healing process. First, Gram staining was used to examine MRSA skin infection on the surface and in deep tissues of the wounds (Fig. 8A). The images of the tissues on day 12 show a purple color, which represents bacterial colonization in the wound, in the untreated and Alg- and Alg-DETA-treated groups. By contrast, the Alg-DETA/NO-treated group showed no bacterial infiltration on and under the skin. In line with the Gram staining results, the Alg-DETA/NO-treated group showed more than a 1-log reduction (~90% killed) in the number of viable bacterial cells on day 6 post-injury (Fig. 8B); there was almost no bacterial burden on day 12 post-injury (>6-log reduction; ~99.9999% killed), which could be explained by the bactericidal effect of NO. The untreated and Alg- and Alg-DETA/NO-treated groups showed no changes in the number of viable bacterial cells; instead, the numbers of bacteria colonizing the wounds increased.

Inflammatory infiltration was quantitatively examined by measuring the activity of MPO, an enzyme that indicates the extent of neutrophil infiltration, and thus, represents the inflammation phase of wound healing (Hasmann et al., 2013). On day 6 post-injury, the Alg-DETA/NO-treated group showed a reduction in MPO activity in the wound tissue compared with that in all other groups (Fig. 8C). On day 12 post-injury, the Alg-DETA/NO-treated group showed a significantly lower MPO activity ($P < 0.05$) than that in the untreated and Alg- and Alg-DETA-treated groups. The direct effect of Alg-DETA/NO on the MPO activity reiterates the fact that NO is a vital molecule that protects against bacterial infection and also influences the functional activity of many immune and inflammatory cell types (e.g., neutrophils) (Tripathi et al., 2007). In particular, NO regulates the migration of polymorphonuclear leukocytes, which are involved in the mediation of inflammatory responses during wound healing via the release of peptides and enzymes, such as MPO (Nolan et al., 2008).

4. Conclusions

We successfully synthesized DETA/NONOate-doped alginate (Alg-

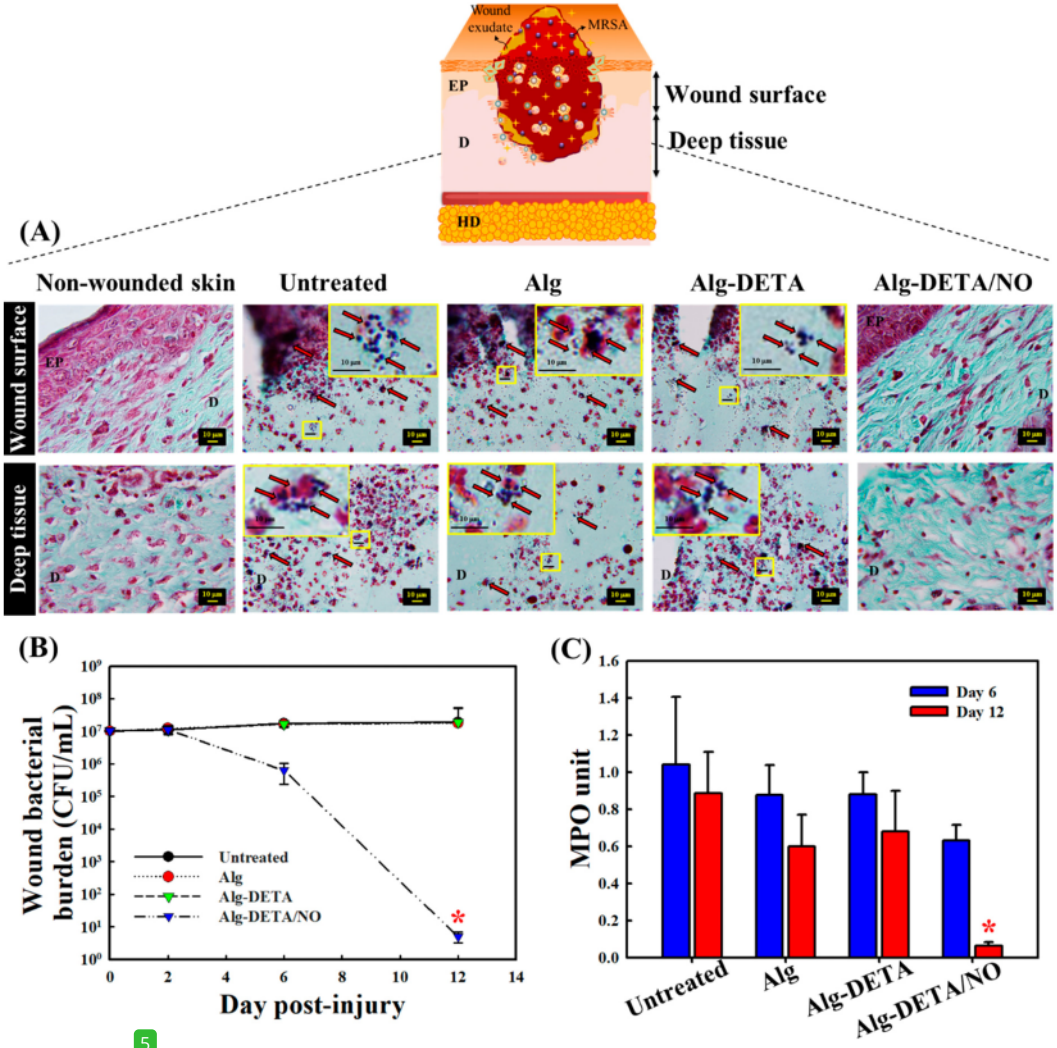

Fig. 8. Bacterial burden in methicillin-resistant *Staphylococcus aureus* (MRSA)-infected wound. (A) Gram staining of skin tissue on the surface of wound. Yellow spots marked with red arrows represent MRSA colonies. (B) Bacteria burden in the wound, determined by counting colony-forming units (CFU) in wound tissues collected on days 2, 6, and 12 after MRSA infection (C) MPO activity on days 6 and 12 post-injury in wound tissues treated with or without Alg-DETA/NO. Data are the mean ± standard deviation ($n = 3$). *$P < 0.05$, compared with the untreated group. Alg, alginate; DETA, diethylenetriamine; NO, nitric oxide.

DETA/NO), which could be transformed into a hydrogel by absorbing wound exudates and showed sustained NO release properties and low cytotoxicity. Alg-DETA/NO exhibited a remarkably prolonged NO release profile over a period of 4 days. Importantly, Alg-DETA/NO showed potent antibacterial activity against MRSA and remarkably lower cytotoxicity toward mouse fibroblasts compared to the free DETA and DETA/NO. Application of Alg-DETA/NO to MRSA-infected wounds resulted in favorable wound healing effects and reduced bacterial infection and inflammation of the wound. Histological examination revealed that wounds treated with Alg-DETA/NO exhibited a healed skin structures similar to that of the healthy epidermis, with increased numbers of fibroblasts and enhanced angiogenesis and collagen deposition. In addition, significantly low MPO activity in the wounds treated with Alg-DETA/NO indicated the absence of prolonged inflammation which is frequently found in chronic wounds. Overall, these results suggest that Alg-DETA/NO could serve as a safe and potent hydrogel dressing for the treatment of MRSA-infected wounds.

CRediT authorship contribution statement

Nurhasni Hasan: Conceptualization, Methodology, Investigation, Formal analysis, Data curation, Writing – original draft, Writing – review & editing, Visualization, Software. **Juho Lee:** Methodology, Investigation, Formal analysis, Software. **Dongmin Kwak:** Methodology, Investigation. **Hyunwoo Kim:** Methodology, Investigation. **Aruzhan Saparbayeva:** Methodology, Investigation. **Hye-Jin Ahn:** Methodology, Data curation. **In-Soo Yoon:** Validation, Writing – review & editing. **Min-Soo Kim:** Validation, Writing – review & editing. **Yunjin Jung:** Validation, Writing – review & editing. **Jin-Wook Yoo:** Conceptualization, Supervision, Funding acquisition, Validation, Data curation, Writing – review & editing.

Declaration of competing interest

There are no conflicts of interest to declare.

Acknowledgements

This work was supported by the Basic Science Research Program through the National Research Foundation of Korea (NRF) funded by the Ministry of Education (No. NRF-2019R1I1A3A01057849).

Appendix A. Supplementary data

Supplementary data to this article can be found online at https://doi.org/10.1016/j.carbpol.2021.118387.

References

Ahonen, M. J. R., Suchyta, D. J., Zhu, H., & Schoenfisch, M. H. (2018). Nitric oxide-releasing alginates. *Biomacromolecules, 19*(4), 1189–1197.

Albaugh, K. W., Biely, S. A., & Cavorsi, J. P. (2013). The effect of a cellulose dressing and topical vancomycin on methicillin-resistant *Staphylococcus aureus* (MRSA) and Gram-positive organisms in chronic wounds: a case series. *Ostomy/Wound Management, 59*(5), 34–43.

Bae, S. H., Bae, Y. C., Nam, S. B., & Choi, S. J. (2012). A skin fixation method for decreasing the influence of wound contraction on wound healing in a rat model. Archives of plastic surgery. *Archives of Plastic Surgery, 39*(5), 457.

Balin, A. K., & Pratt, L. (2002). Dilute povidone-iodine solutions inhibit human skin fibroblast growth. *Dermatologic Surgery, 28*(3), 210–214.

Beauchamp, J. (2010). Infrared Tables (short summary of common absorption frequencies). *Course Notes, 2620*, 19.

Bernkop-Schnürch, A., Kast, C. E., & Richter, M. F. (2001). Improvement in the mucoadhesive properties of alginate by the covalent attachment of cysteine. *Journal of Controlled Release, 71*(3), 277–285.

Blaine, G. (1947). Experimental observations on absorbable alginate products in surgery: gel, film, gauze and foam. *Annals of Surgery, 125*(1), 102.

Blecher, K., Martinez, L. R., Tuckman-Vernon, C., Nacharaju, P., Schairer, D., Chouake, J., … Nosanchuk, J. D. (2012). Nitric oxide-releasing nanoparticles accelerate wound healing in NOD-SCID mice. *Nanomedicine: Nanotechnology, Biology and Medicine, 8*(8), 1364–1371.

Cao, J., Choi, J.-S., Oshi, M. A., Lee, J., Hasan, N., Kim, J., & Yoo, J.-W. (2019). Development of PLGA micro-and nanorods with high capacity of surface ligand conjugation for enhanced targeted delivery. *Asian Journal of Pharmaceutical Sciences, 14*(1), 86–94.

Cao, J., Su, M., Hasan, N., Lee, J., Kwak, D., Kim, D. Y., … Yoo, J.-W. (2020). Nitric oxide-releasing thermoresponsive pluronic F127/alginate hydrogel for enhanced antibacterial activity and accelerated healing of infected wounds. *Pharmaceutics, 12*(10), 926.

Choi, M., Hasan, N., Cao, J., Lee, J., Hlaing, S. P., & Yoo, J.-W. (2020). Chitosan-based nitric oxide-releasing dressing for anti-biofilm and in vivo healing activities in MRSA biofilm-infected wounds. *International Journal of Biological Macromolecules, 142*, 680–692.

Fang, F. C. (1997). Perspectives series: host/pathogen interactions. Mechanisms of nitric oxide-related antimicrobial activity. *The Journal of Clinical Investigation, 99*(12), 2818–2825.

Gansauge, S., Gansauge, F., Nussler, A. K., Rau, B., Poch, B., Schoenberg, M. H., & Beger, H. G. (1997). Exogenous, but not endogenous, nitric oxide increases proliferation rates in senescent human fibroblasts. *FEBS Letters, 410*(2–3), 160–164.

Hasan, N., Cao, J., Lee, J., Naeem, M., Hlaing, S. P., Kim, J., … Yoo, J.-W. (2019). PEI/NONOates-doped PLGA nanoparticles for eradicating methicillin-resistant *Staphylococcus aureus* biofilm in diabetic wounds via binding to the biofilm matrix. *Materials Science and Engineering: C, 103*, Article 109,741.

Hasmann, A., Wehrschütz-Sigl, E., Marold, A., Wiesbauer, H., Schoeftner, R., Geweßler, U., … Binder, B. (2013). Analysis of myeloperoxidase activity in wound fluids as a marker of infection. *Annals of Clinical Biochemistry, 50*(3), 245–254.

Hlaing, S. P., Kim, J., Lee, J., Hasan, N., Cao, J., Naeem, M., … Lee, B.-L. (2018). S-Nitrosoglutathione loaded poly (lactic-*co*-glycolic acid) microparticles for prolonged nitric oxide release and enhanced healing of methicillin-resistant *Staphylococcus aureus*-infected wounds. *European Journal of Pharmaceutics and Biopharmaceutics, 132*, 94–102.

Hudson, N. L. (2020). *NIOSH skin notation (SK) profile: diethylenetriamine (DETA). Infrared Spectroscopy Absorption Table.*(2020).

Keefer, L. K. (2005). Nitric oxide (NO)-and nitroxyl (HNO)-generating diazeniumdiolates (NONOates): emerging commercial opportunities. *Current Topics in Medicinal Chemistry, 5*(7), 625–636.

Kim, S.-J., Kim, J.-S., Papadopoulos, J., Kim, S. W., Maya, M., Zhang, F., … Fidler, I. J. (2009). Circulating monocytes expressing CD31: implications for acute and chronic angiogenesis. *The American Journal of Pathology, 174*(5), 1972–1980.

Kröncke, K.-D., & Suschek, C. V. (2008). Adulterated effects of nitric oxide–generating donors. *Journal of Investigative Dermatology, 128*(2), 258–260.

Lee, J., Hlaing, S. P., Cao, J., Hasan, N., Ahn, H.-J., Song, K.-W., & Yoo, J.-W. (2019). In situ hydrogel-forming/nitric oxide-releasing wound dressing for enhanced antibacterial activity and healing in mice with infected wounds. *Pharmaceutics, 11*(10), 496.

Lee, J., Hlaing, S. P., Cao, J., Hasan, N., & Yoo, J.-W. (2020). In vitro and in vivo evaluation of a novel nitric oxide-releasing ointment for the treatment of methicillin-resistant *Staphylococcus aureus*-infected wounds. *Journal of Pharmaceutical Investigation, 50*, 505–512.

Lee, J., Kwak, D., Kim, H., Kim, J., Hlaing, S. P., Hasan, N., … Yoo, J.-W. (2020). Nitric oxide-releasing S-nitrosoglutathione-conjugated poly (lactic-*co*-glycolic acid) nanoparticles for the treatment of MRSA-infected cutaneous wounds. *Pharmaceutics, 12*(7), 618.

Lee, W. Y., Asadujjaman, M., & Jee, J.-P. (2019). Long acting injectable formulations: The state of the arts and challenges of poly (lactic-*co*-glycolic acid) microsphere, hydrogel, organogel and liquid crystal. *Journal of Pharmaceutical Investigation, 49*(4), 459–476.

Martinez, L. R., Han, G., Chacko, M., Mihu, M. R., Jacobson, M., Gialanella, P., … Friedman, J. M. (2009). Antimicrobial and healing efficacy of sustained release nitric oxide nanoparticles against *Staphylococcus aureus* skin infection. *Journal of Investigative Dermatology, 129*(10), 2463–2469.

Matthews, K., Stevens, H., Auffret, A., Humphrey, M., & Eccleston, G. (2006). Gamma-irradiation of lyophilised wound healing wafers. *International Journal of Pharmaceutics, 313*(1–2), 78–86.

Miller, M., & Megson, I. (2007). Recent developments in nitric oxide donor drugs. *British Journal of Pharmacology, 151*(3), 305–321.

Nolan, S., Dixon, R., Norman, K., Hellewell, P., & Ridger, V. (2008). Nitric oxide regulates neutrophil migration through microparticle formation. *The American Journal of Pathology, 172*(1), 265–273.

Nurhasni, H., Cao, J., Choi, M., Kim, I., Lee, B. L., Jung, Y., & Yoo, J.-W. (2015). Nitric oxide-releasing poly (lactic-*co*-glycolic acid)-polyethylenimine nanoparticles for prolonged nitric oxide release, antibacterial efficacy, and in vivo wound healing activity. *International Journal of Nanomedicine, 10*, 3065.

Oshi, M. A., Naeem, M., Bae, J., Kim, J., Lee, J., Hasan, N., … Yoo, J.-W. (2018). Colon-targeted dexamethasone microcrystals with pH-sensitive chitosan/alginate/Eudragit S multilayers for the treatment of inflammatory bowel disease. *Carbohydrate Polymers, 198*, 434–442.

Privett, B. J., Broadnax, A. D., Bauman, S. J., Riccio, D. A., & Schoenfisch, M. H. (2012). Examination of bacterial resistance to exogenous nitric oxide. *Nitric Oxide, 26*(3), 169–173.

Pyo, H. C., Kim, Y. K., Whang, K. U., Park, Y. L., & Eun, H. C. (1995). A comparative study of cytotoxicity of topical antimicrobials to cultured human keratinocytes and fibroblasts. *Korean Journal of Dermatology, 33*(5), 895–906.

Schlüter, A., Weller, P., Kanaan, O., Nel, I., Heusgen, L., Höing, B., & Dominas, N. (2018). CD31 and VEGF are prognostic biomarkers in early-stage, but not in late-stage, laryngeal squamous cell carcinoma. *BMC Cancer, 18*(1), 1–8.

Shrestha, P., Regmi, S., & Jeong, J.-H. (2020). Injectable hydrogels for islet transplantation: a concise review. *Journal of Pharmaceutical Investigation, 50*(1), 29–45.

Stratton, C. W. (2003). Dead bugs don't mutate: susceptibility issues in the emergence of bacterial resistance. *Emerging Infectious Diseases, 9*(1), 10.

Sun, B., Slomberg, D. L., Chudasama, S. L., Lu, Y., & Schoenfisch, M. H. (2012). Nitric oxide-releasing dendrimers as antibacterial agents. *Biomacromolecules, 13*(10), 3343–3354.

Tian, M., Chen, X., Gu, Z., Li, H., Ma, L., Qi, X., … You, C. (2016). Synthesis and evaluation of oxidation-responsive alginate-deferoxamine conjugates with increased stability and low toxicity. *Carbohydrate Polymers, 144*, 522–530.

Tian, M., Chen, X., Li, H., Ma, L., Gu, Z., Qi, X., … You, C. (2016). Long-term and oxidative-responsive alginate–deferoxamine conjugates with a low toxicity for iron overload. *RSC Advances, 6*(39), 32,471–32,479.

Tripathi, P., Tripathi, P., Kashyap, L., & Singh, V. (2007). The role of nitric oxide in inflammatory reactions. *FEMS Immunology and Medical Microbiology, 51*(3), 443–452.

Van Bambeke, F., Mingeot-Leclercq, M.-P., Struelens, M. J., & Tulkens, P. M. (2008). The bacterial envelope as a target for novel anti-MRSA antibiotics. *Trends in Pharmacological Sciences, 29*(3), 124–134.

Wan, A., Sun, Y., & Li, H. (2008). Characterization of folate-graft-chitosan as a scaffold for nitric oxide release. *International Journal of Biological Macromolecules, 43*(5), 415–421.

White, R. J., Cutting, K., & Kingsley, A. (2006). Topical antimicrobials in the control of wound bioburden. *Ostomy/Wound Management, 52*(8), 26–58.

Wynne, R., Botti, M., Stedman, H., Holsworth, L., Harinos, M., Flavell, O., & Manterfield, C. (2004). Effect of three wound dressings on infection, healing comfort, and cost in patients with sternotomy wounds: a randomized trial. *Chest, 125*(1), 43–49.

22th_Paper_Nurhasni_Hasan_CP_(2021).pdf

ORIGINALITY REPORT

23%	17%	17%	3%
SIMILARITY INDEX	INTERNET SOURCES	PUBLICATIONS	STUDENT PAPERS

PRIMARY SOURCES

1	www.ncbi.nlm.nih.gov Internet Source	3%
2	Nurhasni Hasan, Jiafu Cao, Juho Lee, Shwe Phyu Hlaing et al. "Bacteria-Targeted Clindamycin Loaded Polymeric Nanoparticles: Effect of Surface Charge on Nanoparticle Adhesion to MRSA, Antibacterial Activity, and Wound Healing", Pharmaceutics, 2019 Publication	2%
3	Kim, Jihoon, Yanggy Lee, Kaushik Singha, Hyun Woo Kim, Jae Ho Shin, Seongbong Jo, Dong-Keun Han, and Won Jong Kim. "NONOates–Polyethylenimine Hydrogel for Controlled Nitric Oxide Release and Cell Proliferation Modulation", Bioconjugate Chemistry, 2011. Publication	1%
4	Submitted to Heriot-Watt University Student Paper	1%
5	www.pubmed.pro Internet Source	1%

6	www.spandidos-publications.com Internet Source	1 %
7	studentsrepo.um.edu.my Internet Source	1 %
8	tessera.spandidos-publications.com Internet Source	1 %
9	topsecretapiaccess.dovepress.com Internet Source	<1 %
10	unsworks.unsw.edu.au Internet Source	<1 %
11	www.frontiersin.org Internet Source	<1 %
12	Sara E. Maloney, Kyle V. McGrath, Mona Jasmine R. Ahonen, Daniel S. Soliman et al. "Nitric Oxide-Releasing Hyaluronic Acid as an Antibacterial Agent for Wound Therapy", Biomacromolecules, 2020 Publication	<1 %
13	www.ijpsonline.com Internet Source	<1 %
14	pure.rug.nl Internet Source	<1 %
15	www.ffa.uni-lj.si Internet Source	<1 %

16	patents.google.com Internet Source	<1 %
17	Maarten E A Reith. "Nitric oxide inhibits uptake of dopamine and N-methyl-4-phenylpyridinium (MPP+) but not release of MPP+ in rat C6 glioma cells expressing human dopamine transporter", British Journal of Pharmacology, 12/2002 Publication	<1 %
18	Meng Tian, Xi Chen, Hao Li, Lu Ma, Zhipeng Gu, Xin Qi, Xi Li, Hong Tan, Chao You. "Long-term and oxidative-responsive alginate–deferoxamine conjugates with a low toxicity for iron overload", RSC Advances, 2016 Publication	<1 %
19	www.cog.psy.ruhr-uni-bochum.de Internet Source	<1 %
20	Luis R Martinez. "Antimicrobial and Healing Efficacy of Sustained Release Nitric Oxide Nanoparticles Against Staphylococcus Aureus Skin Infection", Journal of Investigative Dermatology, 04/23/2009 Publication	<1 %
21	mdpi-res.com Internet Source	<1 %
22	www.mdpi.com Internet Source	<1 %

23	Dengyan Wu, Dong Wei, Maotao Du, Song Ming, Qian Ding, Ranjing Tan. "Targeting Antibacterial Effect and Promoting of Skin Wound Healing After Infected with Methicillin-Resistant Staphylococcus aureus for the Novel Polyvinyl Alcohol Nanoparticles", International Journal of Nanomedicine, 2021 Publication	<1 %
24	jultika.oulu.fi Internet Source	<1 %
25	Dong Hoon Shin, Jeong Yeon Jo, Minyoung Choi, Kyung-Hee Kim, Young-Ki Bae, Sang Soo Kim. "Oncogenic KRAS mutation confers chemoresistance by upregulating SIRT1 in non-small cell lung cancer", Research Square Platform LLC, 2023 Publication	<1 %
26	core.ac.uk Internet Source	<1 %
27	epdf.pub Internet Source	<1 %
28	www.freepatentsonline.com Internet Source	<1 %
29	María D. Romero-Sánchez, José Miguel Martín-Martínez. "Treatment of vulcanized styrene-butadiene rubber (SBR) with mixtures	<1 %

of Trichloroisocyanuric Acid and Fumaric Acid", The Journal of Adhesion, 2010
Publication

30	www.e-asct.org Internet Source	<1 %
31	Alexis W. Carpenter, Brittany V. Worley, Danielle L. Slomberg, Mark H. Schoenfisch. "Dual Action Antimicrobials: Nitric Oxide Release from Quaternary Ammonium-Functionalized Silica Nanoparticles", Biomacromolecules, 2012 Publication	<1 %
32	cdr.lib.unc.edu Internet Source	<1 %
33	research.chalmers.se Internet Source	<1 %
34	Pedro Martins da Silva Filho, Alexandre Lopes Andrade, Jessica Barros Arrais Cruz Lopes, Aryane de Azevedo Pinheiro et al. "The biofilm inhibition activity of a NO donor nanosilica with enhanced antibiotics action", International Journal of Pharmaceutics, 2021 Publication	<1 %
35	Ziyang Jia, Yun Luo, Francisco Jose Barba, Yan Wu, Wenping Ding, Shensheng Xiao, Qingyun Lyu, Xuedong Wang, Yang Fu. "Effect of β-cyclodextrins on the physical properties and	<1 %

anti-staling mechanisms of corn starch gels during storage", Carbohydrate Polymers, 2022
Publication

36	Halim, Udayabagya, Chu Ran Zheng, Yu Chen, Zhaoyang Lin, Shan Jiang, Rui Cheng, Yu Huang, and Xiangfeng Duan. "A rational design of cosolvent exfoliation of layered materials by directly probing liquid–solid interaction", Nature Communications, 2013. Publication	<1 %
37	edoc.unibas.ch Internet Source	<1 %
38	www.jri.ir Internet Source	<1 %
39	www.researchsquare.com Internet Source	<1 %
40	Submitted to AUT University Student Paper	<1 %
41	M. Mercedes Pastor-Blas, José Miguel Martín-Martínez, F. J. Boerio. "Influence of Chlorinating Solution Concentration on the Interactions Produced Between Chlorinated Thermoplastic Rubber and Polyurethane Adhesive at the Interface", The Journal of Adhesion, 2010 Publication	<1 %

42	Xinting Cheng, Xibo Pei, Wenjia Xie, Junyu Chen, Yuanyuan Li, Jian Wang, Huile Gao, Qianbing Wan. "pH - Triggered Size - Tunable Silver Nanoparticles: Targeted Aggregation for Effective Bacterial Infection Therapy", Small, 2022 Publication	<1 %
43	d-nb.info Internet Source	<1 %
44	link.springer.com Internet Source	<1 %
45	nanoconvergencejournal.springeropen.com Internet Source	<1 %
46	Submitted to Pusan National University Library Student Paper	<1 %
47	rcastoragev2.blob.core.windows.net Internet Source	<1 %
48	s3-eu-west-1.amazonaws.com Internet Source	<1 %
49	theses.lib.polyu.edu.hk Internet Source	<1 %
50	www.tandfonline.com Internet Source	<1 %
51	cyberleninka.org Internet Source	

		<1 %
52	mafiadoc.com Internet Source	<1 %
53	prr.hec.gov.pk Internet Source	<1 %
54	Tian, Meng, Xi Chen, Zhipeng Gu, Hao Li, Lu Ma, Xin Qi, Hong Tan, and Chao You. "Synthesis and evaluation of oxidation-responsive alginate-deferoxamine conjugates with increased stability and low toxicity", Carbohydrate Polymers, 2016. Publication	<1 %
55	backend.orbit.dtu.dk Internet Source	<1 %
56	eprints.soton.ac.uk Internet Source	<1 %
57	pubag.nal.usda.gov Internet Source	<1 %
58	www.researchgate.net Internet Source	<1 %
59	Dakota J. Suchyta, Mark H. Schoenfisch. " Encapsulation of -Diazeniumdiolates within Liposomes for Enhanced Nitric Oxide Donor Stability and Delivery ", Molecular Pharmaceutics, 2015	<1 %

	Publication	
60	Muhammad Naeem, Junhwan Bae, Murtada A. Oshi, Min-Soo Kim, Hyung Ryong Moon, Bok Luel Lee, Eunok Im, Yunjin Jung, Jin-Wook Yoo. "Colon-targeted delivery of cyclosporine A using dual-functional Eudragit® FS30D/PLGA nanoparticles ameliorates murine experimental colitis", International Journal of Nanomedicine, 2018 Publication	<1 %
61	apps.dtic.mil Internet Source	<1 %
62	blastinjuryresearch.health.mil Internet Source	<1 %
63	docksci.com Internet Source	<1 %
64	docplayer.net Internet Source	<1 %
65	estudogeral.sib.uc.pt Internet Source	<1 %
66	papyrus.bib.umontreal.ca Internet Source	<1 %
67	s-space.snu.ac.kr Internet Source	<1 %
68	www.omicsonline.org Internet Source	<1 %

69	Kaitlyn R. Rouillard, Olivia P. Novak, Alex M. Pistiolis, Lei Yang, Mona J. R. Ahonen, Rebecca A. McDonald, Mark H. Schoenfisch. "Exogenous Nitric Oxide Improves Antibiotic Susceptibility in Resistant Bacteria", ACS Infectious Diseases, 2020 Publication	<1 %
70	Yajie Zhong, Huining Xiao, Farzad Seidi, Yongcan Jin. "Natural Polymer-Based Antimicrobial Hydrogels without Synthetic Antibiotics as Wound Dressings", Biomacromolecules, 2020 Publication	<1 %
71	Kathryn A. Wold, Vinod B. Damodaran, Lucas A. Suazo, Richard A. Bowen, Melissa M. Reynolds. "Fabrication of Biodegradable Polymeric Nanofibers with Covalently Attached NO Donors", ACS Applied Materials & Interfaces, 2012 Publication	<1 %
72	Liu, Guoqiang, Xiaolong Wang, Feng Zhou, and Weimin Liu. "Tuning the Tribological Property with Thermal Sensitive Microgels for Aqueous Lubrication", ACS Applied Materials & Interfaces, 2013. Publication	<1 %
73	Zahra Sadrearhami, Farah Nabilah Shafiee, Kitty K. K. Ho, Naresh Kumar et al.	<1 %

"Antibiofilm Nitric Oxide-Releasing Polydopamine Coatings", ACS Applied Materials & Interfaces, 2019

Publication

Exclude quotes	On	Exclude matches	< 5 words
Exclude bibliography	On		